processes

MDPI

Article

Combining On-Line Characterization Tools with Modern Software Environments for Optimal Operation of Polymerization Processes

Navid Ghadipasha [1], Aryan Geraili [1], Jose A. Romagnoli [1,*], Carlos A. Castor, Jr. [2], Michael F. Drenski [3] and Wayne F. Reed [2]

[1] Department of Chemical Engineering, Louisiana State University, Baton Rouge, LA 70803, USA; nghadi1@lsu.edu (N.G.); agerai1@lsu.edu (A.G.)
[2] Department of Physics and Engineering Physics, Tulane University, New Orleans, LA 70118, USA; ccastorj@tulane.edu (C.A.C.); wreed@tulane.edu (W.F.R.)
[3] Advanced Polymer Monitoring Technologies, Inc., New Orleans, LA 70125, USA; michael.drenski@apmtinc.com
* Correspondence: jose@lsu.edu; Tel.: +1-225-578-1377

Academic Editor: Masoud Soroush
Received: 6 December 2015; Accepted: 5 February 2016; Published: 15 February 2016

Abstract: This paper discusses the initial steps towards the formulation and implementation of a generic and flexible model centric framework for integrated simulation, estimation, optimization and feedback control of polymerization processes. For the first time it combines the powerful capabilities of the automatic continuous on-line monitoring of polymerization system (ACOMP), with a modern simulation, estimation and optimization software environment towards an integrated scheme for the optimal operation of polymeric processes. An initial validation of the framework was performed for modelling and optimization using literature data, illustrating the flexibility of the method to apply under different systems and conditions. Subsequently, off-line capabilities of the system were fully tested experimentally for model validations, parameter estimation and process optimization using ACOMP data. Experimental results are provided for free radical solution polymerization of methyl methacrylate.

Keywords: free radical polymerization; molar mass distribution; dynamic optimization; parameter estimation; online monitoring

1. Introduction

In the polymer industry, batch and semi-batch reactors are widely used for the production of different classes of polymers. There is considerable economic incentive to develop real-time optimal operating policies that will result in the production of polymers with desired molecular properties. In the case of polymerization processes, the molar mass distribution (MMD) of a polymer is one of the most important quality control variables since many of the polymer end-use properties are directly dependent on the MMD. Some examples include the mechanical properties such as stiffness, strength and viscoelasticity [1–3]. Optimal operation in polymerization usually involves computing and accurately maintaining the optimal policies that can lead to a product with desired MMD and final conversion, while minimizing the total operation time. However, direct feedback control of MMD is difficult to achieve due to several reasons. The primary issue is the lack of on-line promising method for monitoring polymer properties. Monitoring requires continuous measurement of the reacting solution to make data available for closed-loop control or state estimation of the system. The ability to monitor polymerization reactions as they occur is necessary to ensure fulfillment of

the proposed recipe. Most of the control strategies in the literature for polymeric systems are based on open-loop methods which heavily depend on the accuracy of the mathematical model and will produce unsatisfactory results in case of disturbances in the system.

An extensive amount of work for feedback control of polymerization systems has been reported during last decades, most using an inferential technique to infer the polymer properties. Guyot *et al.* [4] used an on-line gas chromatographic analysis of the monomer mixture to control the copolymer composition in emulsion polymerization. Dimitratos *et al.* [5,6] developed a feedforward-feedback control strategy based on the use of an extended Kalman filter for state estimation. The Kalman filter method is based on a linear approximation of the nonlinear process [7] but has problems with stability and convergence [8–11]. For that reason many nonlinear methods have been developed. Hammori *et al.* [7] developed a nonlinear state observer that uses rate generation due to chemical reaction to obtain key parameters during free radical copolymerization. This technique is simpler to tune than Kalman filters. Kravaris *et al.* [12] utilized a general nonlinear feedforward-feedback control strategy based on temperature tracking to control copolymer composition. In order to control the nonlinear systems Model predictive control (MPC) [13–18] has been suggested. The main disadvantage of the MPC is that it cannot explicitly deal with plant model uncertainties.

Common manipulated variables in polymerization processes include coolant or heating medium flow rates, gas or liquid flow rates for pressure control, feed rate of monomer, solvent, or initiator, and agitator speed [19]. Crowley *et al.* [20] introduced a new method for controlling the weight chain length distribution of polymer in batch free radical polymerization processes by manipulating temperature. Although temperature has a considerable effect on MMD, when the reaction is extremely exothermic, which is the case in many polymerization systems, changing temperature is not an efficient way to control MMD. In this case, MMD is controlled by manipulating the ratio of monomer to initiator or adding a chain transfer agent. This will give the extra degree of freedom to minimize the operation time and also conversion of monomer. The combined control of temperature and reagent flow has been studied by Ellis *et al.* [21]. They proposed a MMD estimator based on an extended Kalman filter to provide current estimates of the entire MMD based on measurements of monomer conversion obtained by on-line densitometry and periodic time delayed measurements of MMD from on-line size-exclusion chromatograph. Simultaneous change of temperature and monomer addition to control MMD was investigated and it was demonstrated that the proposed feedback control strategy is effective in rejecting disturbances. In general, controlling molar mass is best achieved by manipulating the monomer, initiator and chain transfer agent concentration [5,22,23].

More recently a platform for automatic continuous online monitoring of polymerization (ACOMP) was proposed [24]. ACOMP allows for automatic, continuous and model independent monitoring of polymerization reactions. It uses continuous dilution of a small stream from the reactor, in conjunction with light scattering, viscosity, ultraviolet absorption and refractometric detectors. This provides monomer and co-monomer conversion, weight average molar mass, weight average intrinsic viscosity, average composition drift and distribution, and certain measures of polydispersity [24,25]. The ability to monitor polymerization reactions as they occur brings several benefits. First, following kinetics and other reaction characteristics allows fundamental understanding of reaction mechanisms that can help accelerate the development of new polymer chemistries and processes. Second, monitoring the effects of changing reaction conditions, such as temperature, reagent types, and concentration, provides a concise means for bench scale or small pilot reaction optimization.

This paper discusses the initial steps towards the formulation and implementation of a generic and flexible model-based framework for integrated simulation, estimation, optimization and feedback control of polymerization systems. The emphasis is on developing a comprehensive scheme which can be applied for the optimal operation of various polymeric systems and this was achieved by combining the powerful capabilities of the on-line monitoring system, ACOMP, with a modern simulation, estimation and optimization software environment. Using literature data, an initial validation of the framework for a number of cases of simulation and optimization is presented. This shows the

flexibility of the method to work under different systems and conditions. Subsequently, the off-line capabilities of the framework were fully tested experimentally for model validations, parameter estimation as well as for process optimization. Starting with kinetic information from literature a new set of kinetic parameters were obtained for our case study as well as confidence intervals for the estimated parameters. This illustrates the importance of this strategy to follow kinetics and other reaction characteristics allowing fundamental understanding of reaction mechanisms that can help in the development of new polymer chemistries and processes. An offline model-based optimization analysis was conducted and experimentally validated to determine the optimal temperature profile in conjunction with the optimal monomer and initiator flow rate in order to reach a final target polymer while minimizing the batch time. A brief analysis on the controllability of the system under feedback conditions was also performed through a combination of simulation and experimental work.

2. Model Centric Framework

A shortcoming of using advanced operating and control strategies in polymerization processes is the unavailability of sensors able to determine online process status and provide corrective actions. The ACOMP platform will provide a leap towards integration of monitoring, control, and optimization tools in the control of complex industrial polymerization [26]. The proposed structure will forge initial links between ACOMP and advanced modelling and control principles and demonstrate unprecedented feedback control of polymerization reactions. The final goal is a self-contained intelligent system for advanced operation of polymerization processes where both ACOMP and the software environment exchange data seamless toward achieving target final products.

The conceptual representation of the aforementioned framework for integrated simulation, estimation, optimization and feedback control of systems is illustrated in Figure 1. The modelling work was carried out using gPROMS modelling language (V4.1.0, Process Systems Enterprise Inc London, United Kingdom, 2015), providing a complete environment for modelling/analysis of complex systems. Among gPROMS other advantages are: (a) modelling and solution power; (b) multiple activities using the same model; (c) integrated steady state and dynamic capabilities; (d) parameter estimation potentials; (e) sophisticated optimization tools; and (f) structural model information for advanced process control implementations. The parameter estimation entity makes use of the data gathered from the experimental runs. It has the ability to estimate an unlimited number of parameters, using data from multiple dynamic experiments and ability to specify different variance models among the variables as well as among the different experiments. The optimization entity allows for the typical dynamic optimization problems arising from batch and/or semibatch operation to be formulated and implemented. One of the key issues is the connectivity of the software platform with the control system and ACOMP towards full integration. In this specific application gPROMS would need to be started from an external application and data will travel back and forth. An approach for this is to use the gSERVER API, transforming the application into the so-called gPROMS-based Application, or gBA or as an alternative via gO:RUN-xml. Both of these as well as open platform communication are currently explore in our experimental facilities.

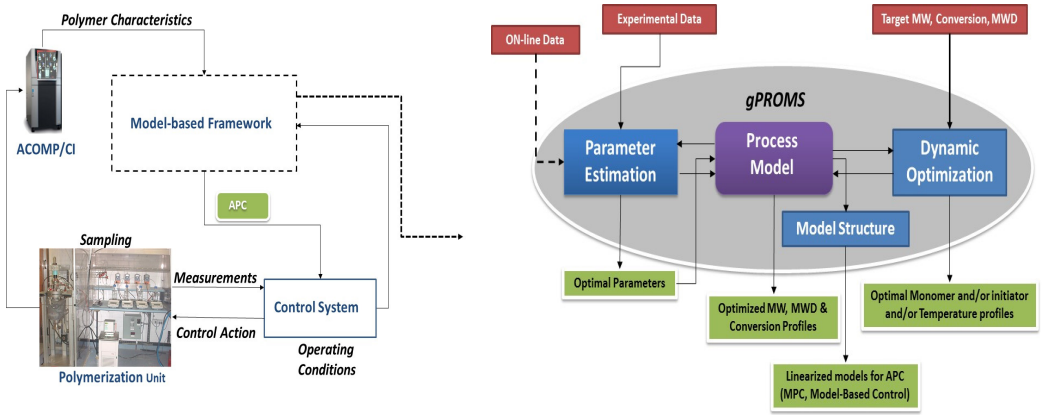

Figure 1. Schematic of the integrated simulation, estimation, optimization and feedback control of polymerization systems.

2.1. Process Modelling

Modelling of polymerization processes is the other significant issue which plays a key role in the development of model-based control strategies. A number of well-known models have been introduced with much attention on the control of number and weight average molar mass [27,28]. Although weight average molar mass is usually the most important parameter in characterization of the polymer chain length distribution, there are cases in which controlling average properties may not be sufficient. For example, when a broad or bimodal distribution is desired [29]. A very attractive approach to characterize chain length distribution in batch free radical polymerization reactor has been presented by Crowley *et al.* [30,31]. This technique applies the method of finite molecular weight moments in conjunction with the kinetic rate equations to calculate the weight chain length distribution. As it was illustrated, it is feasible to control MMD in a batch polymerization process [20]. The modelling approach in this work incorporates the method of moment to obtain chain length distribution directly from the kinetic equations and includes the free volume theory to calculate the initiator efficiency, termination and propagation rate. As a first trial, a detailed mechanistic model for solution polymerization of methyl methacrylate (MMA) in batch and semi-batch reactors is developed and tested. This case study was selected since ample information regarding the kinetic mechanisms and data for MMA polymerization was available in the literature thus allowing faster prototyping. However, more complex systems will be considered in the future.

2.1.1. Reaction Mechanisms and Kinetic Equations

The reaction mechanisms adopted consists of three important steps: Initiation, propagation and termination. Chain transfer to monomer and solvent were also incorporated for better prediction of the molar mass. The detailed mechanism is as follow:

Initiation

$$I \xrightarrow{k_d} 2R \tag{1}$$

$$R + M \xrightarrow{k_i} P_1 \tag{2}$$

Propagation

$$P_n + M \xrightarrow{k_p} P_{n+1} \tag{3}$$

Chain transfer to monomer and solvent

$$P_n + M \xrightarrow{k_{fm}} D_n + P_1 \tag{4}$$

$$P_n + S \xrightarrow{k_{fs}} D_n + P_1 \tag{5}$$

Termination

$$P_n + P_m \xrightarrow{k_{tc}} D_{n+m} \tag{6}$$

$$P_n + P_m \xrightarrow{k_{td}} D_n + D_m \tag{7}$$

where I denotes the initiator, R is the primary initiator radical, M is the monomer, S is the solvent and P_j and D_j are the corresponding growing live polymer radical and dead polymer. Under standard assumptions such as well-mixed reactor, quasi steady state assumptions (for the radicals) and long chain hypothesis, the following set of kinetic and dynamic equations describe the system:

$$\frac{dN_m}{dt} = -\left(k_p + k_{fm}\right) P_0 N_m + F_m C_{mf} - F_{out} C_m \tag{8}$$

$$\frac{dN_i}{dt} = -k_d N_i + F_i C_{if} - F_{out} C_i \tag{9}$$

$$\frac{dN_s}{dt} = -k_{fs} N_s P_0 + F_i C_{sif} + F_m C_{smf} - F_{out} C_s \tag{10}$$

$$\frac{d\left(\lambda_0 V\right)}{dt} = \left(k_{fm} N_m + k_{td} P_0 V + k_{fs} N_s\right) \alpha P_0 + \frac{1}{2} k_{tc} P_0^2 V \tag{11}$$

$$\frac{d\left(\lambda_1 V\right)}{dt} = \left[\left(k_{fm} N_m + k_{td} P_0 V + k_{fs} N_s\right)\left(2\alpha - \alpha^2\right) + k_{tc} P_0 N\right] \frac{P_0}{(1-\alpha)} \tag{12}$$

$$\frac{d\left(\lambda_2 V\right)}{dt} = \left[\left(k_{fm} N_m + k_{td} P_0 V + k_{fs} N_s\right)\left(\alpha^3 - 3\alpha^2 + 4\alpha\right) + k_{tc} P_0 V \left(\alpha + 2\right) \frac{P_0}{(1-\alpha)}\right] \frac{P_0}{(1-\alpha)^2} \tag{13}$$

where $N_m = C_m V$, $N_i = C_i V$, $N_s = C_s V$

$$\alpha = \frac{k_p C_m}{k_p C_m + k_{fm} C_m + k_{fs} C_s + k_{tc} P_0 + k_{td} P_0} \tag{14}$$

$$P_0 = \sqrt{\frac{2 f C_i k_d}{k_{tc} + k_{td}}} \tag{15}$$

$$V = \left[1 - \frac{\lambda_1 w_m}{\rho_p}\right]^{-1} \left[\frac{N_m w_m}{\rho_m} + \frac{N_s w_s}{\rho_s} + \frac{N_i w_i}{\rho_i}\right] \tag{16}$$

Here C_m, C_i and C_s represent the concentrations of monomer, initiator and solvent in the reactor, respectively. V illustrates the volume of the content of the reactor, F_m and F_i are the volumetric flow rate of monomer and initiator respectively which are fed into the reactor in the semi batch mode. F_{out} is the constant flow rate out of the reactor for the ACOMP extraction stream. C_{mf}, C_{if}, C_{sif} and C_{smf} are the concentration of monomer in the monomer feed stream, the initiator in the initiator feed stream and solvent in the initiator and monomer flow stream. P_0 is the total concentration of live polymer which is obtained from the quasi steady state assumption. λ_0, λ_1 and λ_2 are the corresponding moments for the dead polymers, and α is the probability of propagation. f is the initiator efficiency and ρ_m, ρ_i, ρ_s and ρ_p are the densities of the monomer, initiator, solvent and polymer which are temperature dependent. k_p, k_d, k_{fm}, k_{fs}, k_{tc} and k_{td} are the propagation, initiation, chain transfer to monomer, chain transfer to solvent, termination by combination and termination by disproportionation rate. Kinetic rate constants are all temperature dependent functions based on Arrhenius equation [28] and as we will see due to strong nonlinearity of the MMA system, the propagation and termination rate depend on conversion as well.

The conversion of the monomer is defined as the number of moles of monomer reacted in the tank divided by the total amount of monomer which has been loaded initially in the reactor and added by the semi-batch flow:

$$X = \frac{N_{m0} + \int_0^t F_m C_{mf} dt - C_m V - \int_0^t F_{out} C_m dt}{N_{m0} + \int_0^t F_m C_{mf} dt} \tag{17}$$

Here, N_{m0} is the initial amount of monomer in the reactor. Number average and weight average molar mass of the polymers are calculated by considering only the moment of dead polymers and neglecting the live polymer concentration which is valid for low and medium conversions when the concentration of live polymer is negligible.

$$M_n = w_m \frac{\lambda_1}{\lambda_0},\ M_w = w_m \frac{\lambda_2}{\lambda_1} \tag{18}$$

2.1.2. Formalism for Gel, Glass and Cage Effects in MMA Polymerization

In free radical polymerization, the mobility of the radicals decreases along the reaction due to increase in the viscosity of the reactor as more polymers are produced. This phenomenon which is called "gel effect" causes a reduction in the termination rate constant k_t, and should be considered in the formulation of the model. At high conversion when even the motion of monomer is severely restricted the propagation rate k_p, is also decreased. This glassy state in which the solution is highly viscous sets a limiting conversion on the polymerization process. In this work the correlation by [28,32] is used for both gel and glass effect. This can be written as:

$$g_t = \begin{cases} 0.10575 \exp\left(17.15 v_f - 0.01715\left(T - 273.15\right)\right), & v_f > v_{ftc} \\ 2.3 \times 10^{-6} \exp\left(75 v_f\right), & v_f \leqslant v_{ftc} \end{cases} \tag{19}$$

$$g_p = \begin{cases} 1, & v_f > v_{fpc} \\ 7.1 \times 10^{-5} \exp\left(171.53 v_f\right), & v_f \leqslant v_{fpc} \end{cases} \tag{20}$$

Here, v_{ftc} and v_{fpc} are the critical free volumes which are calculated as below:

$$v_{ftc} = 0.1856 - 2.965 \times 10^{-4}\left(T - 273.15\right) \tag{21}$$

$$v_{fpc} = 0.05 \tag{22}$$

v_f is the total free volume which is given by:

$$v_f = \phi_m v_{fm} + \phi_s v_{fs} + \phi_p v_{fp} \tag{23}$$

where

$$v_{fi} = 0.025 + \alpha_i\left(T - T_{gi}\right) \tag{24}$$

φ_i and T_{gi} are the volume fraction and the glass transition temperature of the polymer, solvent and monomer and α_i is a constant. The values of the parameter for this case are shown in Table 1 [28]. For butyl acetate the corresponding glass transition temperature was considered as an adjustable parameter which has to be determined by parameter estimation.

Table 1. Parameters for Methyl methacrylate gel and glass affect correlations.

Parameter	MMA	Poly Methyl Methacrylate	Butyl Acetate
α	0.001	0.00048	0.001
T_g(K)	167	387	#

The initiator efficiency f, appearing in Equation (15) describes the fraction of initiator free radicals which can successfully initiate the polymerization. Not all primary radicals can produce propagating chains. They execute many oscillations in "cages" before they diffuse apart and initiate a reaction. During the oscillations the radicals may also form an inactive species. Therefore, to account for the two competing phenomena, initiator efficiency is appended in the mathematical model. Initiator efficiency factor also decreases as the viscosity of the reactor solution rises. The free volume theory is used to model this relationship:

$$f = f_0 \exp\left(-C\left(\frac{1}{V_\mathrm{f}} - \frac{1}{V_\mathrm{fcr}}\right)\right) \tag{25}$$

where f_0 is the initial initiator efficiency and C is a constant with the values of 0.53 and 0.006 for Azobisisobutyronitrile Fan *et al.* [33].

2.1.3. Molar Mass Distribution

In order to obtain complete representation of molecular weight distribution, a similar methodology proposed by Crowley *et al.* [30] based on finite weight fractions is applied with modifications for dealing with semi-batch operations. This method consists of dividing the entire polymer population into discrete intervals and calculating the weight fraction of polymer in each of the discrete intervals. By ignoring the concentration of live polymer, given that it is negligible compared with the dead polymer concentration, for each interval of (m,n) the polymer weight fraction is calculated with the following equations:

$$f(m,n) = \frac{\sum_{i=m}^{n} iD_\mathrm{i}V}{\sum_{i=2}^{\infty} iD_\mathrm{i}V} \text{ Or } f(m,n) = \frac{\sum_{i=m}^{n} iD_\mathrm{i}V}{\lambda_1 V} \tag{26}$$

The dynamic of weight fraction can then be obtained as:

$$\frac{d\,f(m,n)}{dt} = \frac{1}{\lambda_1 V}\sum_{i=m}^{n} i\frac{d\,(D_\mathrm{i}V)}{dt} - \frac{1}{\lambda_1 V} f(m,n)\,\frac{d\,(\lambda_1 V)}{dt} \tag{27}$$

where the right-hand side of Equation (27) represents the dynamic growth of dead polymers of length n which can be written according to the kinetic rate equation as below:

$$\frac{d\,(D_\mathrm{i}V)}{dt} = \left[k_\mathrm{fm}C_\mathrm{m} + k_\mathrm{fs}C_\mathrm{s} + k_\mathrm{td}C_\mathrm{p}\right] P_\mathrm{n} V \tag{28}$$

This can be shown by further simplification as follows:

$$\frac{d\,(D_\mathrm{i}V)}{dt} = k_\mathrm{p}C_\mathrm{m}VP_\mathrm{i}\frac{(1-\alpha)}{\alpha} \tag{29}$$

Substituting equation (29) into (27) we get:

$$\frac{d\,f(m,n)}{dt} = \frac{1}{\lambda_1 V}\,k_\mathrm{p}C_\mathrm{m}V\frac{(1-\alpha)}{\alpha}\sum_{i=m}^{n} iP_\mathrm{i} - \frac{1}{\lambda_1 V} f(m,n)\,\frac{d\,(\lambda_1 V)}{dt} \tag{30}$$

The term $\sum_{i=m}^{n} iP_\mathrm{i}$ can be represented as:

$$\sum_{i=m}^{n} iP_\mathrm{i} = \sum_{i=m}^{\infty} iP_\mathrm{i} - \sum_{i=n+1}^{\infty} iP_\mathrm{i} \tag{31}$$

Assuming, $P_\mathrm{n} = \alpha P_{n-1}$ and $P_\mathrm{n} = (1-\alpha)\alpha^{n-1}P$:

$$\sum_{i=m}^{\infty} iP_\mathrm{i} = \left[\frac{m\,(1-\alpha)+\alpha}{(1-\alpha)}\right]\alpha^{\mathrm{m}-1}P - \left[\frac{(n+1)\,(1-\alpha)+\alpha}{(1-\alpha)}\right]\alpha^{\mathrm{n}}P \tag{32}$$

And the final form of weight fraction for a semi-batch condition will be:

$$\frac{d\,f\,(m,n)}{dt} = \frac{1}{\lambda_1} k_{\mathrm{p}} C_{\mathrm{m}} \left(\left[\frac{m\,(1-\alpha)+\alpha}{\alpha} \right] \alpha^{\mathrm{m}-1} - \left[\frac{(n+1)\,(1-\alpha)+\alpha}{\alpha} \right] \alpha^{\mathrm{n}} \right) P - \frac{1}{\lambda_1 V} f\,(m,n)\,\frac{d\,(\lambda_1 V)}{dt} \quad (33)$$

2.1.4. Energy Balances

One of the most complex features of the free radical polymerization is the exothermic nature of the reaction. Generated energy during polymerization should be removed by a coolant or dissipated to environment. Otherwise, the reactor can thermally run away. Even if run away does not occur, molar mass distribution can broaden. To model non-isothermal polymerization, energy balance should be applied to the reactant mixture in the reactor and oil in the bath. From the application of the energy conservation principle, the following equations show the energy balance for a perfectly mixed jacketed semi-batch reactor:

$$\frac{d\left(\rho_{\mathrm{r}} C_{\mathrm{pr}} V T_{\mathrm{r}}\right)}{dt} = (-\Delta \mathrm{H})\,(k_{\mathrm{p}} + k_{\mathrm{fm}}) N_{\mathrm{m}} \times C_{\mathrm{p}} - UA\left(T_{\mathrm{r}} - T_{\mathrm{j}}\right) + \left(F_{\mathrm{m}} \rho_{\mathrm{m}} C_{\mathrm{pm}} + F_{\mathrm{i}} \rho_{\mathrm{s}} C_{\mathrm{ps}}\right)\left(T_{\mathrm{f}} - T_{\mathrm{r}}\right) \quad (34)$$

$$\frac{d\left(\rho_{\mathrm{j}} C_{\mathrm{pj}} V_{\mathrm{j}} T_{\mathrm{j}}\right)}{dt} = F_{\mathrm{j}} \rho_{\mathrm{j}} C_{\mathrm{pj}}\left(T_{\mathrm{j},0} - T_{\mathrm{j}}\right) + UA\left(T_{\mathrm{r}} - T_{\mathrm{j}}\right) \quad (35)$$

Here T_{r} and T_{j} denote the reactor and jacket temperature respectively. It was assumed that both reactor and jacket are perfectly mixed and have a constant temperature. ρ_{r} and C_{pr} are the average density and specific heat capacity of the reactor. C_{pm}, C_{ps} and C_{pj} are the specific heat capacity of monomer, solvent and coolant flow which consists of water and ethylene glycol. U is the overall heat transfer coefficient and A is the heat transfer area.

2.2. Parameter Estimation

Kinetic rate constants are significant parameters of a polymerization reaction which have to be determined accurately since even a slight change in them will result in considerable difference of the final polymer characteristics. The data regarding the kinetic rate constants may be obtained from literature or determined experimentally. However for some materials the properties are not available in the literature and it may not be possible to measure them through experiments due to lack of experimental facilities. Moreover, there are many criteria that affect the kinetic rate parameters such as reactor operating conditions, presence of inhibitors and purity of the materials which are different for various systems. So, proper values of the rate constants should be determined via a parameter estimation technique. This is an important prerequisite step in order to evaluate these variables and improve the model reliability for optimization and model-based control scheme development.

The parameter estimation is often formulated as an optimization problem in which the estimation attempts to determine the values for the unknown parameters in order to maximize the probability that the mathematical model will predict the values obtained from the experiments. Effective solution of parameter estimation is attainable if the following criteria are met [34]:

(a) The nonlinear system should be structurally identifiable which means that each set of parameter values will result in unique output trajectories.

(b) Parameters which have a weak effect on the estimated measured variables and the parameters which their effect on the measured output is linearly dependent should be detected and removed from the formulation of the estimation since their effect cannot be either accurately or individually quantified.

For the proposed system the parameters of the polymerization model that was introduced in section 2.1 can be represented as $z(t) = [X(t), M_{\mathrm{w}}(t)]$ which are the outputs of the parameter estimation model, $u(t) = [T(t), F_{\mathrm{m}}(t), F_i(t)]$ which are the time-varying inputs and θ the set of model parameters to be estimated which in this case are $[A_{\mathrm{d}}, A_{\mathrm{p}}, A_{\mathrm{td}}, f_0, T_{\mathrm{gs}}]$. A_{d}, A_{p} and A_{td} are the pre exponential factors

of the decomposition rate, propagation rate and termination rate respectively. The selection of these parameters are justified as the most sensitivity in conversion and weight average molar mass data is with respect to the termination and propagation rate of a polymeric chain. Proper estimation of the initiator efficiency factor is also important since it controls the effective radical concentration. Since the transition temperature for butyl acetate is not available in the literature this parameter should also be estimated. In this work the parameter estimation scheme is based on maximum likelihood criterion. The gEST function in gPROMS is used as the software to estimate the set of parameters using the data gathered from the different experimental runs. Each experiment is characterized by a set of conditions under which it is performed, which are:

1. The overall duration.
2. The initial conditions which are the initial loading of initiator, solvent and monomer.
3. The variation of the control variables. For the batch experiment temperature is the only variable, while in semi batch both temperature and flow rate of monomer and/or initiator have to be considered.
4. The values of the time invariant parameters.

Assuming independent, normally distributed measurement errors, ϵ_{ijk} with zero means and standard deviations, σ_{ijk} this maximum likelihood goal can be captured through the following objective function:

$$\phi = \frac{N}{2}\ln(2\pi) + \frac{1}{2}\min_{\theta}\left\{\sum_{i=1}^{NE}\sum_{j=1}^{NV_i}\sum_{k=1}^{NM_{ij}}\left[\ln\left(\sigma_{ijk}^2\right) + \frac{\left(\tilde{z}_{ijk} - z_{ijk}\right)^2}{\sigma_{ijk}^2}\right]\right\} \tag{36}$$

where N describes the total number of measurements taken during all the experiments, θ is the set of model parameters to be estimated which may be subjected to a given lower and upper bound, NE, NV_i and NM_{ij} are respectively the total number of experiments performed, the number of variables measured in the ith experiment and the number of measurements of the jth variable in the ith experiment. σ_{ijk}^2 is the variance of the kth measurement of variable j in experiment i while $\tilde{z}_{ijk}$ is the kth measured value of variable j in experiment i and z_{ijk} is the kth model-predicted value of variable j in experiment i.

According to [35] the variable σ_{ijk}^2 depends on the error structure of the data which can be constant (homoscedastic) or depend on the magnitude of the predicted and measured variables (heteroscedastic). If σ_{ijk}^2 is fixed in the model the maximum likelihood problem is reduced into a least square criterion. If a purely heteroscedastic model applied the error has the following structure:

$$\sigma_{ijk}^2 = \omega_{ijk}^2\left(\tilde{z}_{ijk}\right)^{\gamma} \tag{37}$$

This means that as the magnitude of the measured variable increases the variance of $\tilde{z}_{ijk}$ also increases. The parameter ω_{ijk}^2 and γ are determined as part of the optimization during the estimation. In this work we assume the measurement error for both conversion and weight average molecular weight in all the experiments can be described by constant variance models since the errors for both conversion and weight average molecular weight is independent of their magnitude in the measurement. The given upper and lower bounds of the variance are based on the accuracy of the measurement plant and the function gEST specifies the ω_{ijk}^2 value along with X and M_w as part of the optimization.

2.3. Dynamic Optimization

The objective of the dynamic optimization is to find the optimal control profile for one or more control variables and control parameters of the system that drives the process to the desired final

polymer property while minimizing the reaction time. The process control variables conform to their impact on the product quality and their capability for real time implementation. In this case temperature, monomer and initiator flow rate were selected as the control variables. Temperature plays a very important role in controlling the reaction kinetics which have a considerable impact on the molecular weight distribution while monomer and initiator flowrates are also a powerful means of controlling molar mass by affecting the concentration of the main feed to the reactor. The optimization of the model was performed using the gOPT function in gPROMS that applies the control vector parameterization (CVP) approach. Variation of the control variables in this case is considered as piecewise-constant, indicating the control variables remain constant at a certain value over a certain part of the time horizon before they jump discreetly to a different value over the next interval. The optimization algorithm determines the values of the controls over each interval, as well as the duration of the interval. Optimizer implements a "single-shooting" dynamic optimization algorithm consists of the following steps:

1. Duration of each control interval and the values during the interval are selected by the optimizer
2. Starting from the initial condition the dynamic system is solved in order to calculate the time-variation of the states of the system
3. Based on the solution, the values of the objective function and its sensitivity to the control variables and also the constraints are determined.
4. The optimizer revises the choices at the first step and the procedure is repeated until the convergence to the optimum condition is achieved.

For the proposed system the general optimal control problem is formulated as:

$$\min_{t_f, u(t), v} J\left(t_f\right) \tag{38}$$

Subjected to the process model and the following constraints:

$$x\left(t_0\right) - x_0 = 0 \tag{39}$$

$$t_f^{min} \leqslant t_f \leqslant t_f^{max} \tag{40}$$

$$u^{\min} \leqslant u\left(t\right) \leqslant u^{\max} \tag{41}$$

$$v^{\min} \leqslant v\left(t_f\right) \leqslant v^{\max} \tag{42}$$

where J for the general case is defined as:

$$J = w_1\left(\frac{X_f}{X_t} - 1\right)^2 + w_2\left(\frac{M_{w,f}}{M_{w,t}} - 1\right)^2 + w_3\sum_{i=1}^{nc}\left(\frac{f_{i,f}}{f_{i,t}} - 1\right)^2 + w_4\left(\frac{t_f}{t_t} - 1\right)^2 \tag{43}$$

Here x_0 is the initial condition of the system including the initial loading in the reactor and t_f stands for the time horizon while $u(t)$ indicates the control variables which are the temperature, monomer and initiator flow rates subjected to their lower and upper bounds. v_t represents the time variant parameters being the volume of the contents of the reactor. The formulation of the objective function consists of four terms. X_f, $M_{w,f}$ and $f_{i,f}$ are the values of the monomer conversion, molar mass and weight fraction of polymer within a chain length at the final time t_f respectively and X_t, $M_{w,t}$ and $f_{i,t}$ are their corresponding desired values. w_1–w_4 are the weighting factors, determining the significance of each term in the objective function. A schematic representation of the optimization problem for the polymerization problem is given in Figure 2.

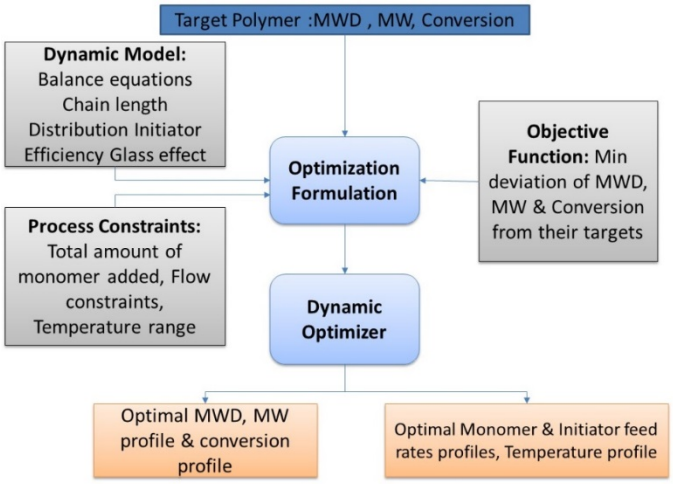

Figure 2. Schematic representation of the optimization problem in polymerization processes.

3. Experimental System

The methyl methacrylate monomer stabilized with 20 ppm of hydroquinone was supplied by Sigma-Aldrich. The Azo initiator, azobisizobutyronitrile (AIBN) was supplied by Sigma-Aldrich. Butyl acetate (BA) was used as solvent for the polymerization reactions and was supplied by Sigma-Aldrich. Nitrogen gas (N2) was supplied by Air Gas S.A. as an ultra-pure gas and used to keep the inert atmosphere inside the reactor. Acetone with minimum purity of 99.5% was supplied by Sigma-Aldrich and used to clean the reactor.

3.1. Experimental Apparatus—ACOMP System

Batch and Semi Bach solution polymerization reactions were conducted in the experimental setup shown in Figure 3. The reactor shown is a 540 mL cylindrical round-bottom glass reactor (Radleys, Shire Hill, Essex, United Kingdom), equipped with a double walled cooling jacket and reflux condenser. Agitation of the reactor (Custom Made at Tulane University PolyRMC, New Orleans, LA, USA) was done with a U-anchor style impeller driven by an overhead stirring motor (IKA Works, Inc., Wilmington, NC, USA). The reactor temperature was controlled with the aid of a thermostatic bath and a thermocouple (Huber USA, Inc., Cary, NC, USA) connected to a data acquisition system (Brookhaven Instruments Corp., Holtsville, NY, USA). The reflux condenser (Radleys, Shire Hill, Essex, United Kingdom), connected to a chilled thermostatic bath was used to prevent loss of reactants. To allow for continuous extraction of the reactor contents, the solution was circulated from the bottom of the reactor by a Zenith 9000 series gear pump (Colfax Corporation, Annapolis Junction, MD, USA) at 15 mL/min. From this circulation line a small stream was pulled by a Knauer high pressure isocratic pump (ICON Scientific Inc., North Potomac, MD, USA) and transferred to the first of two mixing chambers for dilution and conditioning of the polymer sample. This first stage of dilution is done under atmospheric pressure to allow for degassing of trapped air in the polymer stream. The now diluted and quenched polymer is again extracted by a Shimadzu LC-10ADvp isocratic pump (Shimadzu Scientific Instruments, Houston, TX, USA) and further diluted into a static mixing tee (Idex U-466S), (IDEX Health & Science LLC., Oak Harbor, WA, USA). Solvent inflow for both mixing chambers was provided by multiple Shimadzu LC-10ADvp isocratic pumps (Shimadzu Scientific Instruments, Houston, TX, USA). Now that the polymer stream has been thoroughly quenched, diluted and conditioned in the ACOMP "Front End" to a concentration level sufficient for intrinsic measurements, it is flowed through a series of detectors designated as the ACOMP "Detector Train". These detectors monitor the absolute properties of the polymer throughout the entire polymerization process.

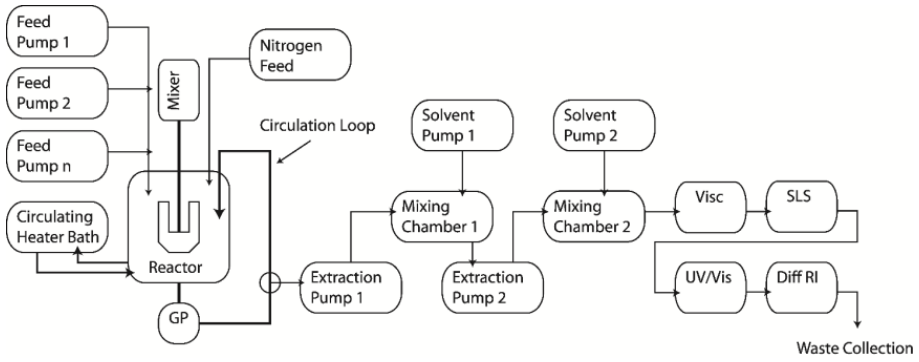

Figure 3. Automatic continuous on-line monitoring of polymerization setup for the monitoring of methyl methacrylate solution polymerization used in this work.

The diluted sample stream now flows through a custom built single capillary viscometer (Custom Made at Tulane University PolyRMC, New Orleans, LA, USA), a Brookhaven Instrument BI-MwA multi-angle scattering photometer (Brookhaven Instruments Corp., Holtsville, NY, USA) (operating with a vertically polarized diode laser beam at 660 nm vacuum wavelength), a Shimadzu SPD-10AV dual wavelength UV/visible spectrophotometer (Shimadzu Scientific Instruments, Houston, TX, USA) and a Shimadzu RID-10A differential refractometer (Shimadzu Scientific Instruments, Houston, TX, USA). The signal from each instrument and the output of the reactor thermocouple were all digitized by A/D inputs on the BI-MwA input module, which contained 16 input channels working at 24 bit resolution. The UV wavelengths used was 269 nm. The viscometer used a capillary of length 10 cm and internal diameter of 0.02 in.

3.2. Experimental Procedure

The solvent in the reactor was purged with nitrogen at least 30 min prior to beginning the reaction. Before beginning the reaction, pure solvent (BA) was pumped at 2.0 mL/min through the entire detectors train (UV, RI, *etc.*) to obtain the baseline for each instrument. After stabilization of the detector baselines by pure solvent, the MMA (monomer) baseline was established by withdrawing from the reactor at 0.3 mL/min, and mixing with solvent at the mixing chamber. The flow rates of both the pure solvent from reservoir and that one from the reactor (containing the reaction mixture) used in this phase were 2.0 and 0.2 mL/min, respectively. Providing a dilution ratio of 1:10. In all of the experiments, the total flow rate was set at 2.0 mL/min and the diluted solution always reached the detector train at a temperature of 25 °C. After baseline stabilization for MMA the AIBN was added to initiate the reaction.

4. Results and Discussion

In this section, model predictions are compared with the literature data and experiments which have been performed using ACOMP system. The results are illustrated in terms of the conversion history and the evolution of molar mass and molar mass distribution. In the first case the proposed model is tested under a different system of initiator and solvent. The model is then verified against experimental data where the polymerization of methyl methacrylate using butyl acetate as solvent and AIBN as the initiator is considered.

4.1. Validation Using Literature Data

The experimental data provided by Crowley *et al.* [31] is used to investigates the applicability of the proposed framework. Batch free radical solution polymerization of methyl methacrylate has been carried out in a 4 L jacketed stirred tank reactor which was initially charged with 500 mL of MMA, 500 mL of ethyl acetate solvent, and 9 g of 2,2¢-azobis(2-methylbutanenitrile) initiator. The reactor was

heated to 65 °C, regulated at that temperature to 27% monomer conversion, and then the temperature was decreased to 50 °C to intentionally broaden the molecular weight distribution. Results from the paper and simulation from the model are represented below for the conversion and molecular weight distribution at the end of the batch. As can be observed in Figure 4 they are in quite good agreement.

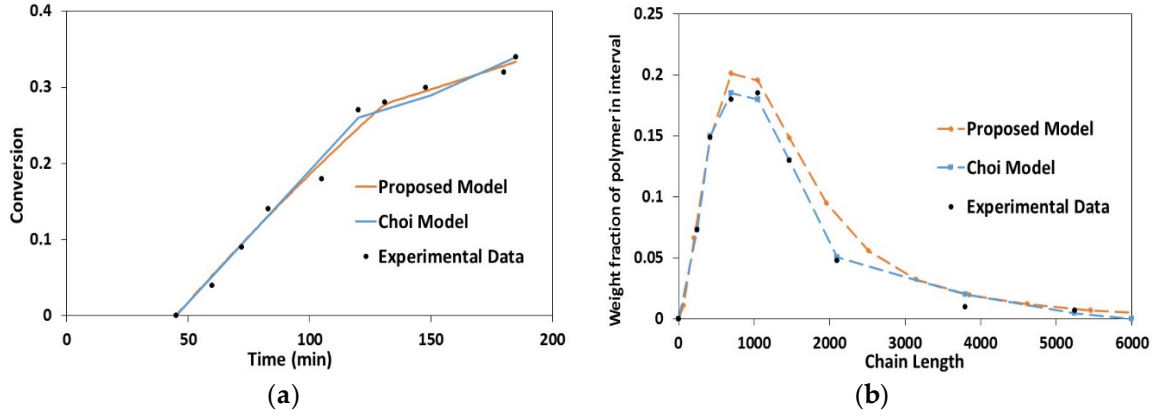

Figure 4. Comparison between model simulations and literature results. (**a**) Panel-Conversion profile. (**b**) Panel-Molar mass distribution at the end of the batch.

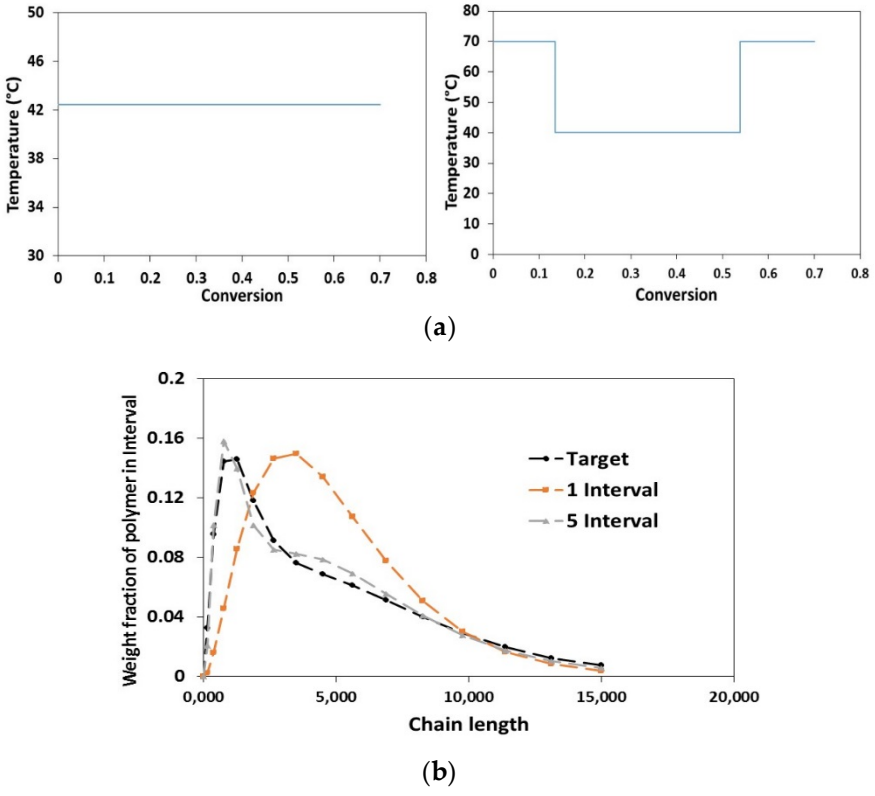

Figure 5. Optimization results: (**a**) Temperature profiles; (**b**) Molar mass distribution.

Data from Crowley *et al.* [31] was also utilized for the optimal batch operation. Based on the developed model it is possible to obtain the optimal trajectory of the temperature which lead to the desired molar mass distribution of polymers. The main problem in the batch optimization is the final time which is not specified. The proposed solution is to set all the kinetic equations with respect to conversion since its final value has already been specified. The solution of the optimization is a

temperature profile with respect to conversion. The profile can then be implemented and the state of the system is monitored with respect to time. The objective now is to reach this final distribution by manipulating temperature before we reach the specified monomer conversion which is 0.7 in this case. There are two criteria that affect the results of the optimization. First, the number of intervals for the monomer conversion and second the initial guess for the temperature profile. Here the results obtained by manipulating the number of intervals are presented. Results for 1 and 5 intervals are provided in Figure 5, which illustrates the MMD for each case, as compared with the target. The results are in good agreement with those obtained in the original paper.

4.2. Experimental Validation for Batch and Semi-Batch Free Radical Polymerization of MMA Using Butyl Acetate as Solvent and AIBN Initiator

The experimental set-up discussed above was employed in this case to fully validate the proposed strategy for both batch and semibatch operation; Up to now previous works in the literature had been based on infrequent and incomplete sets of data and/or limited to batch operation. In this work model validations and parameter estimation have been carried out using ACOMP data. The capability of the model to properly describe the polymerization system has been investigated by doing a number of experiments in both semi-batch and batch mode using different trajectories for temperature and initiator and monomer flow rate. Conversion, weight average molar mass as well as molar mass distribution trajectories along the whole process were evaluated.

In an initial step, using a set of the experimental data, parameter estimation was performed for the main kinetic parameters. The optimal values of the estimated parameters as well as the uncertainty of the parameter represented as 95% confidence interval (CI) are shown in Table 2. Here, the contours correspond to a confidence level of 95%. In other words, there is a probability of 95% that the true values of the parameter pair fall within this ellipsoidal confidence region that is centered in the parameter estimates. In addition to confidence intervals the correlation matrix is also represented in Table 3 as a 5 × 5 lower triangular matrix (the upper triangular matrix is identical to the lower one). The most pronounced correlations between the parameters are shown in bold.

Table 2. Original and estimated value of the kinetic rate parameters for the free radical polymerization of MMA (first iteration).

Parameter	Description	Original Value	Estimated Value	Confidence Interval			95% *t*-value	Standard Deviation
				90%	95%	99%		
A_d	Decomposition (1/min)	1.58×10^{15}	1.37×10^{15}	1.25×10^{14}	1.49×10^{14}	1.96×10^{14}	9.19	7.60×10^{13}
A_p	Propagation (m^3/mol·min)	4.2×10^5	9×10^5	5.23×10^4	6.23×10^4	8.20×10^4	14.43	3.17×10^4
A_{td}	Termination [m^3/mol·min]	1.06×10^8	4.56×10^8	5.97×10^7	7.12×10^7	9.37×10^7	6.40	3.63×10^7
f_0	Initial Initiator Efficiency	0.58	0.57	0.048	0.057	0.076	9.84	0.029
T_s	Solvent Transition Temperature (K)	181	142.61	0.539	0.6431	0.84	221.7	0.327

Table 3. Correlation matrix for the estimated parameters of the system.

Estimated Parameters	A_d	A_p	A_t	f_0	T_s
A_d	1	-	-	-	-
A_p	**0.117**	1	-	-	-
A_t	**0.111**	0.988	1	-	-
f_0	–0.988	**0.038**	**0.043**	1	-
T_s	**0.104**	**0.179**	**0.233**	**–0.070**	1

Most of the estimated parameters obtained have narrow confidence intervals indicating that the number of measurements performed for the parameter estimation were sufficient. The normalized covariance matrix shows that although a few parameters are quite correlated, most parameters estimated in the optimization are only weakly correlated and therefore are suitable for being estimated simultaneously. Larger correlation coefficients are found between the propagation rate and the termination rate as well as initial initiator efficiency and decomposition rate as shown in Figure 6. Likely, any change in one of these parameters could be compensated by a change in the other ones. For example, the coefficient between A_p and A_{td} is 0.94 indicating a strong correlation between them and making it difficult to find a unique estimate for these parameters. Unique parameter estimate means that the parameters have an acceptably low correlation to any of the other parameters and a low confidence interval. Thus, in spite of the large covariance mentioned above, a consistent estimation is possible because of the true value of the estimated parameters are located within a very small confidence bands reducing their uncertainty. However, the confidence ellipsoids are large including in most cases negative numbers. Therefore, a second iteration was performed by eliminating two of the correlated parameters A_d and A_{td} and fixing their values to the estimated ones in the first iteration. The optimal values of the estimated parameters as well as the uncertainty of the parameter represented as 95% confidence interval (CI) are shown in Table 4.

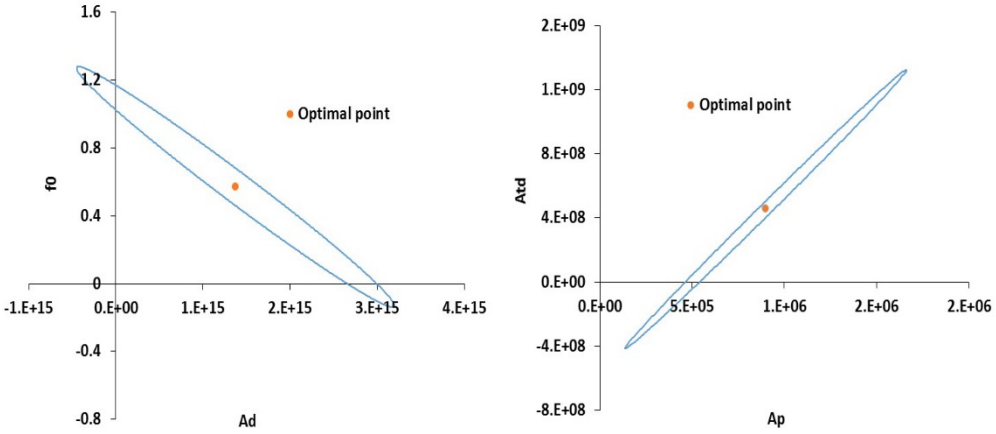

Figure 6. Confidence ellipsoids for A_d–f_0 and A_p–A_t.

Table 4. Original and estimated value of the kinetic rate parameters (second iteration) for the free radical polymerization of MMA.

Parameter	Description	Original Value	Estimated Value	Confidence Interval			95% *t*-value	Standard Deviation
				90%	95%	99%		
A_p	Propagation Rate (m^3/mol·min)	3×10^5	8.5×10^5	2547	3035	3993	280.1	1546
f_0	Initial Initiator Efficiency	0.58	0.56	0.001166	0.0013	0.00182	403.2	0.00073
T_s	Solvent Transition Temperature (K)	142	149.94	0.3906	0.465	0.6123	322.2	0.237

For purposes of illustration the confidence regions for the parameter pairs estimated are shown in Figure 7. None of the confidence ellipsoids cross either the x or y axes. Thus, no parameter pair has a parameter value equal to zero. The confidence ellipsoids also show small negative correlation between propagation constant and corresponding glass transition temperature for the solvent.

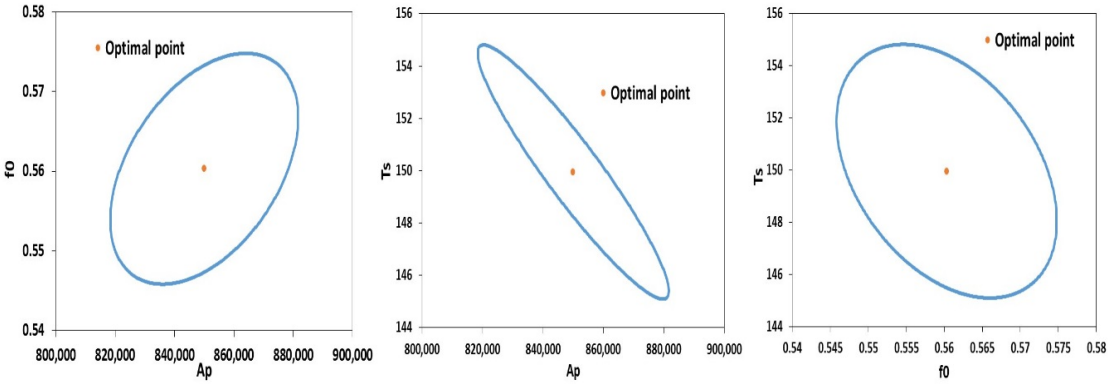

Figure 7. Confidence ellipsoids for final estimated parameters.

Figure 8 shows the conversion and molar mass profiles for two batch conditions with constant and varying temperature. As can be observed, the parameter estimation significantly improves the results. The simulation results after the parameter estimation have an excellent agreement with the experimental data for both conditions, indicating the adjusted model has good predictive capabilities for the proposed system.

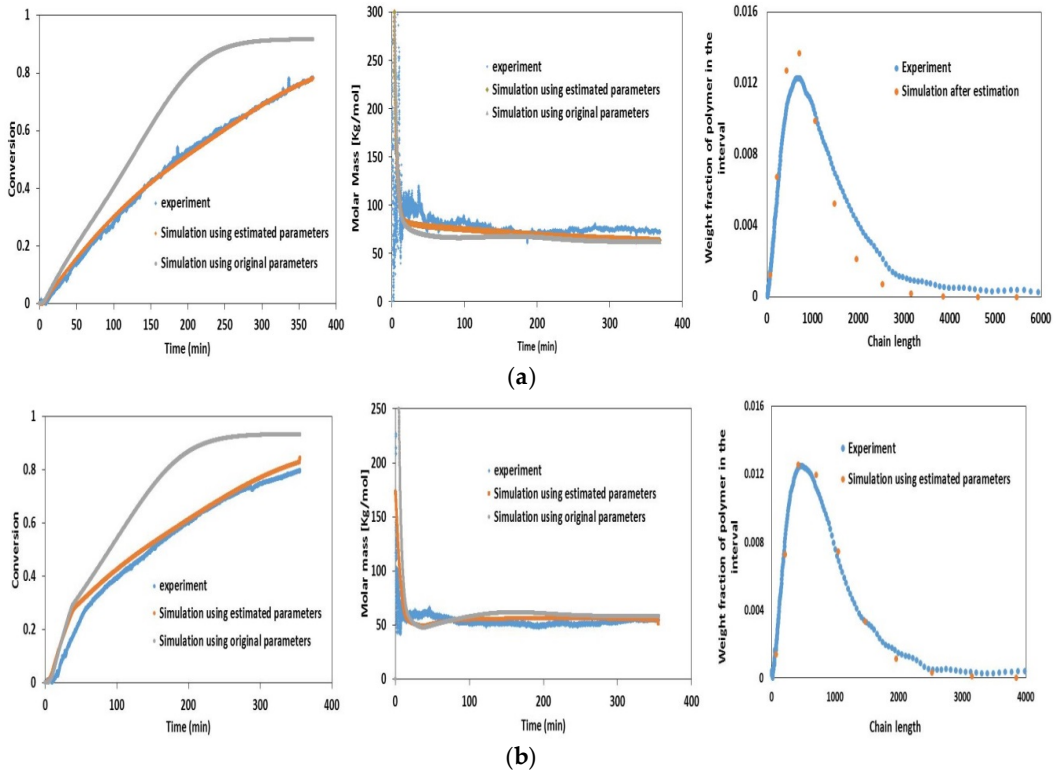

Figure 8. Comparison between experimental data and simulation with original and estimated parameters: (**a**) Isothermal experiment; (**b**) Non-isothermal experiment.

Next, the adjusted model is embedded into the optimization environment to investigate alternative optimal operational policies for final target products. Two objective functions were formulated. One is to determine the optimal trajectories of the control input values that minimize the reaction time while the product qualities reach the specification at the end of the process and the other will only consider the product properties at the end of the process given enough time to the reaction. The optimizer iteratively computes the sequence of reactor temperature, monomer and initiator flow rates which

will yield the best match between the final conversion, molar mass and molar mass distribution and their corresponding target values. Figure 9 presents a snapshot of the three selected iterations. The graph on the left-hand side shows the conversion profile and the right diagram represents the calculated objective function values. Since the solution for early iterations are not optimal the final objective function is high and there is a large discrepancy in the final conversion. Simulation results of optimal profiles at final iteration are shown in Figure 10 for the three control variables and as can be observed there is an excellent agreement between the final values and the target suggesting the advantage of using reagent and monomer flow with temperature to control not only the conversion and weight average molecular weight but also the complete distribution. It should be noted that the optimizer, CVP-S (Control Vector Parameterization- Single Shooting), used by gPROMS may find the local minima rather than the global one. So, the solution is sensitive to the initial point and it is necessary to properly initialize the optimization problem in order to capture the global minima in case of local minima existence.

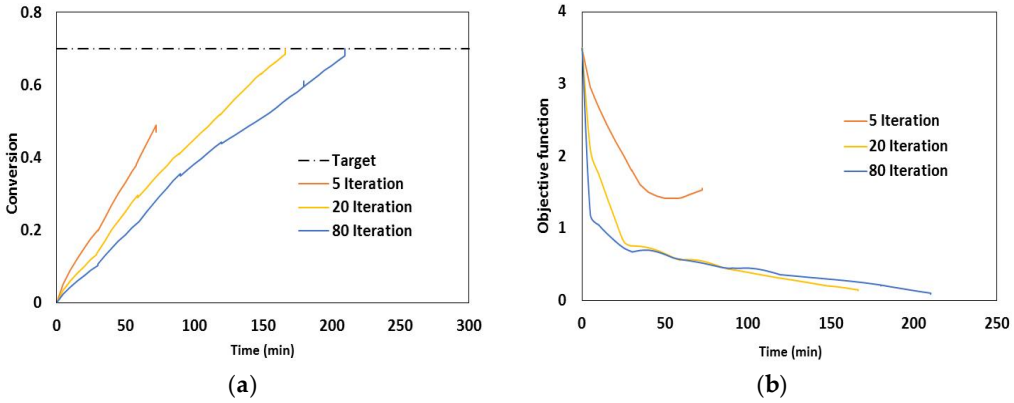

Figure 9. Conversion (**a**) and objective function (**b**) profiles at three different iterations.

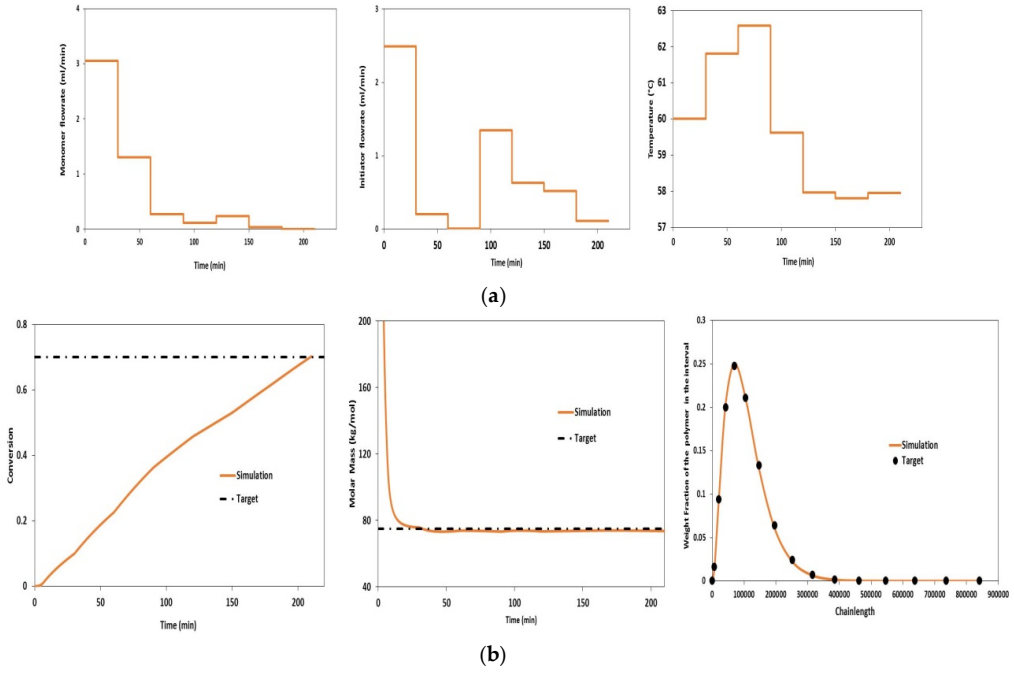

Figure 10. Simulation results of the optimal trajectories considering time in the objective function: (**a**) Input (manipulated) variables; (**b**) Controlled variables (targets).

To demonstrate the feasibility of the proposed optimization strategy the second optimization algorithm for the objective function has been validated also experimentally using data from ACOMP. Table 5 provides the values of the different parameters and the constraints used in this experiment. Temperature and flow constraints are used based on the capacity of the pump and jacket while the minimum volume constraint is the minimum necessary volume for the sensors to have a good estimation of the reactor condition. Figure 11 shows the resulting optimal trajectories of the input variables (temperature, monomer and initiator flows) with the validation results in terms of the model predictions (targets) and the experimental data when the obtained inputs trajectories are applied into the experimental systems. The complete distribution has been shown at the final time of the experiment. The maximum deviations from the model simulation is in the order of 0.03 for conversion and 5 kg/mol for the molar mass. The final distribution is also in a very good agreement with the model predictions showing the feasibility of the proposed scheme.

Table 5. Values of optimization constraints parameters.

Variable	Value	Unit
N_{m}	0.5	mol
N_{s}	0.5	mol
N_{i}	0.01	mol
$F_{\max}$	5	mL/min
$F_{\min}$	0	mL/min
$T_{\max}$	70	°C
$T_{\min}$	50	°C
$V_{\max}$	500	mL
$V_{\min}$	100	mL

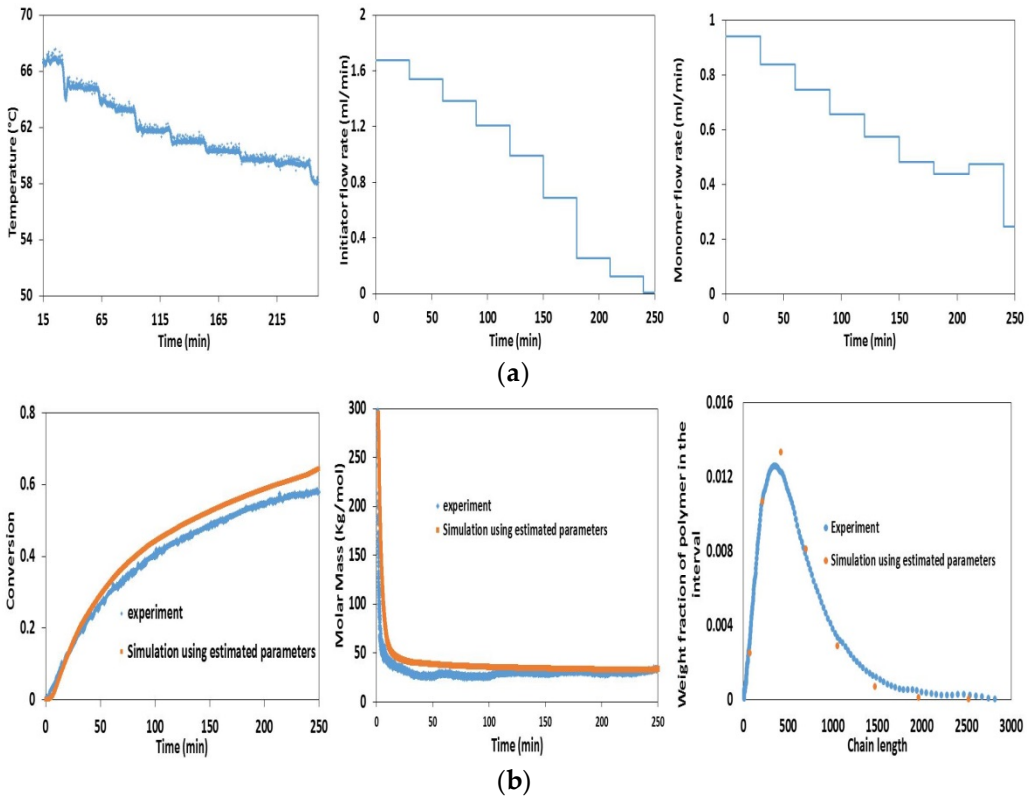

Figure 11. Validation of optimal runs: (**a**) Input (manipulated) variables; (**b**) Controlled variables (targets).

To analyze the controllability of the system under feedback control and as a preliminary step towards the on-line feedback control implementation, a number of simulations combined with experimental information were performed. In this study, the experimental data from the optimal semi-batch operation for the corresponding controlled variable was used as a set-point in a simulated feedback scheme. In this way the experimental optimal profiles for conversion (in the single loop case) and experimental optimal profiles of both conversion and molar mass flow (in the multi-loop case) were provided to the simulator/controller to adjust the temperature and both temperature and initiator flow to achieve the targets. The adjusted input trajectories are then compared to the experimental ones showing the necessary adjustments needed for the control system to care for the model uncertainties. The objective in this part is to propose a straightforward modification to the open-loop optimal recipe described above that will allow the process to meet the optimal condition under non-ideal process circumstances.

The block diagram of the proposed structure is shown in Figure 12. The three possible manipulated variables in this case are the temperature, monomer and initiator flow rate. In the single loop approach, two of the possible manipulated variables still follow the same optimal recipe while the other variable changes based on a PI-like control algorithm in order to follow exactly the set point trajectory. In this case conversion has been selected as the control variable and its controllability with respect to the reactor temperature is investigated. The temperature adjusted using a cascade control system which has been represented schematically in Figure 13. The approach followed here is to start the operation in an open-loop fashion and switch to feedback control during the batch operation. The switching time is around 20 min for the single loop and 60 min for the multi loop controller. Figure 14 shows the performance of the closed loop system. As can be seen good control of the conversion through the batch operation was attained by slight modifications of the open-loop optimal trajectories as predicted from the optimization step. However the molar mass is still out of specifications with respect to the desired final value.

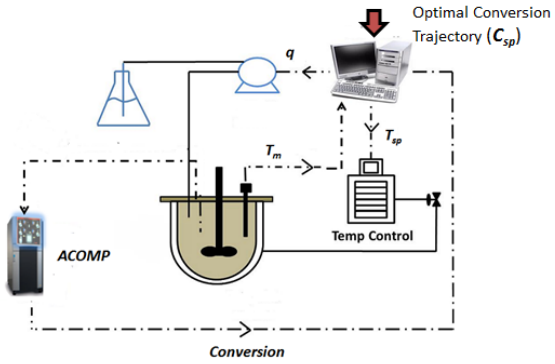

Figure 12. Schematic of apparatus and sensors for the proposed control strategy.

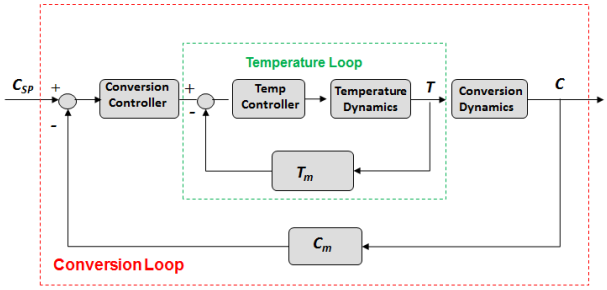

Figure 13. Schematic of cascade control for conversion.

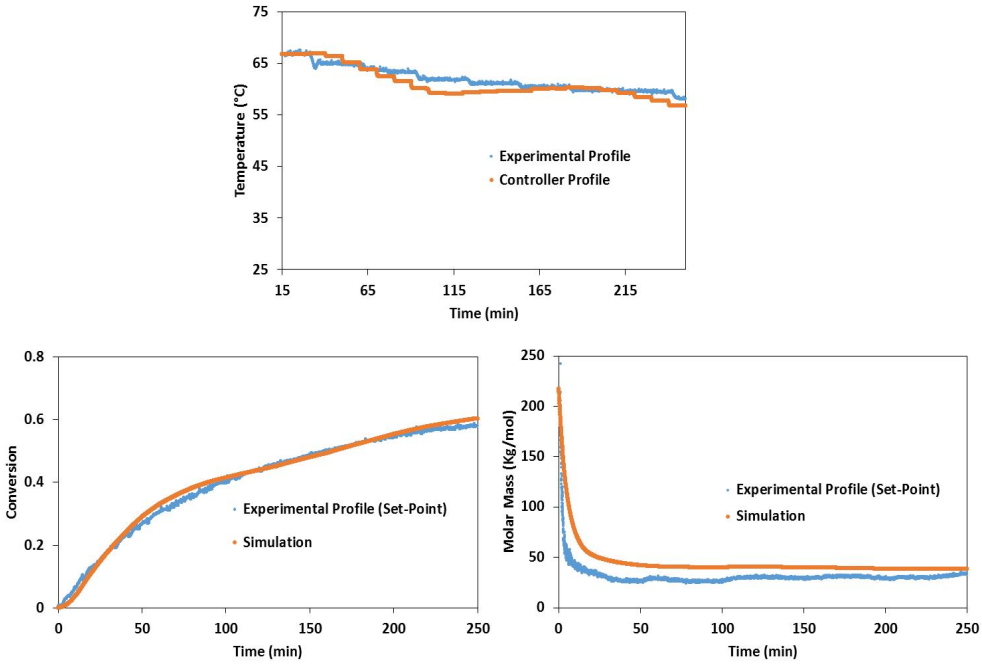

Figure 14. Closed-loop results using single loop controller.

In the multi-loop approach the conversion was again controlled using the cascade configuration as described above but an additional loop was added by adjusting the initiator flow to control the molar mass. Figure 15 illustrates how both conversion and molar mass trajectories follow exactly the desired values as indicated in the plot. One should notice however that small corrections in the molecular weight requires a large control action (initiator flow) indicating low sensitivity of the manipulated variable with respect to the control variable. Also, the interaction between the two loops can be appreciated since the temperature and conversion profiles are slightly modified with respect to the single loop case. Specially during the first action of the initiator controller.

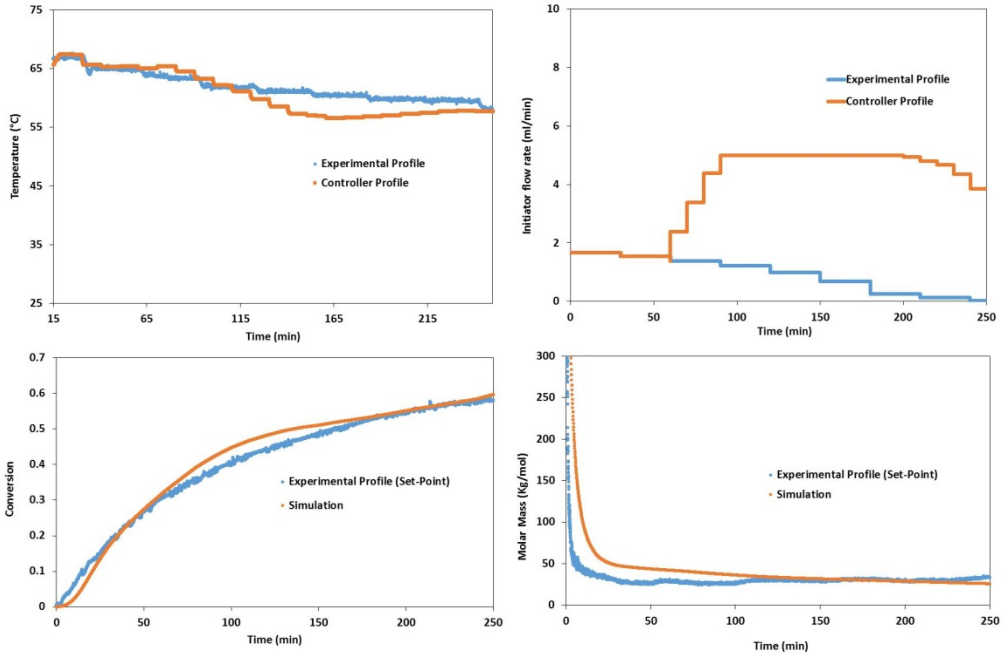

Figure 15. Closed-loop results for multi-loop controllers.

5. Conclusions

Formulation and implementation of a model-based framework for prediction and understanding of free radical polymerization processes has been dealt in this paper. The proposed framework is based on the recent development in characterizing molecular weight distribution (MWD) in polymerization processes combined with a state-of–the art experimental tools for on-line monitoring of polymeric properties towards the optimal operations of this type of systems. The method of finite molecular weight moments has been proposed to represent MWD. This allows computation of the complete chain length distribution instead of molecular weight averages. The model presented was modified for application in semi batch processes. The parameters of the kinetic model were then identified and estimated for the case study of MMA free radical polymerization. Dynamic optimization of the system using the CVP technique was undertaken to yield a product with desired polymer molecular weight characteristics in terms of monomer conversion, weight average molecular weight and the entire desired molecular weight distribution. The model-based optimal policy was validated experimentally and fair to good results were achieved. Preliminary feedback control algorithms were implemented and tested through simulations to achieve a desired conversion and weight average molecular weight of the system. They included single-loop and multi-loop Proportinal-Integral control strategies.

Building on these results, current efforts focus on developing the potential and expanding the capabilities of this new on-line measuring method and modelling approach to fully characterize and control the dynamics involved in polymerization systems. Incorporating advanced control policies with an on line execution level controller and application to other polymerization processes will be the subject of the forthcoming paper.

Acknowledgments: The authors acknowledge support from United States Department of Energy, Advanced Manufacturing Office, DE-EE0005776 and the National Science Foundation under the NSF EPSCoR Cooperative Agreement No. EPS-1430280 with additional support from the Louisiana Board of Regents.

Author Contributions: Navid Ghadipasha and Aryan Geraili conceived the programming and design algorithm for modelling, simulation, estimation, optimization and control part under Jose A. Romagnoli's supervision. The experiments were designed and performed by Michael F. Drenski and Carlos A. Castor under Wayne F. Reed's Supervision. The section "Experimental system" was written by Michael F. Drenski. Navid Ghadipasha wrote the other sections while everyone supervised the writing process.

Conflicts of Interest: The authors declare no conflict of interest.

References

1. Wu, T.; Yu, L.; Cao, Y.; Yang, F.; Xiang, M. Effect of molecular weight distribution on rheological, crystallization and mechanical properties of polyethylene-100 pipe resins. *J. Polym. Res.* **2013**, *20*, 1–10. [CrossRef]
2. Schimmel, K.H.; Heinrich, G. The influence of the molecular-weight distribution of network chains on the mechanical-properties of polymer networks. *Colloid Polym. Sci.* **1991**, *269*, 1003–1012. [CrossRef]
3. Malekmotiei, L.; Samadi-Dooki, A.; Voyiadjis, G.Z. Nanoindentation study of yielding and plasticity of poly(methyl methacrylate). *Macromolecules* **2015**, *48*, 5348–5357. [CrossRef]
4. Guyot, A.; Guillot, J.; Pichot, C.; Guerrero, L.R. New design for production of constant composition co-polymers in emulsion polymerization—Comparison with co-polymers produced in batch. *Abstr. Pap. Am. Chem. S* **1980**, *180*, 131–ORPL.
5. Dimitratos, J.; Georgakis, C.; Elaasser, M.S.; Klein, A. Dynamic modeling and state estimation for an emulsion copolymerization reactor. *Comput. Chem. Eng.* **1989**, *13*, 21–33. [CrossRef]
6. Dimitratos, J.; Georgakis, C.; Elaasser, M.; Klein, A. An experimental-study of adaptive kalman filtering in emulsion copolymerization. *Chem. Eng. Sci.* **1991**, *46*, 3203–3218. [CrossRef]
7. Hammouri, H.; McKenna, T.F.; Othman, S. Applications of nonlinear observers and control: Improving productivity and control of free radical solution copolymerization. *Ind. Eng. Chem. Res.* **1999**, *38*, 4815–4824. [CrossRef]
8. Dochain, D.; Pauss, A. Online estimation of microbial specific growth-rates—An illustrative case-study. *Can. J. Chem. Eng.* **1988**, *66*, 626–631. [CrossRef]

9. Kozub, D.J.; Macgregor, J.F. State estimation for semibatch polymerization reactors. *Chem. Eng. Sci.* **1992**, *47*, 1047–1062. [CrossRef]
10. Mutha, R.K.; Cluett, W.R.; Penlidis, A. On-line nonlinear model-based estimation and control of a polymer reactor. *Aiche. J.* **1997**, *43*, 3042–3058. [CrossRef]
11. Mutha, R.K.; Cluett, W.R.; Penlidis, A. A new multirate-measurement-based estimator: Emulsion copolymerization batch reactor case study. *Ind. Eng. Chem. Res.* **1997**, *36*, 1036–1047. [CrossRef]
12. Kravaris, C.; Wright, R.A.; Carrier, J.F. Nonlinear controllers for trajectory tracking in batch processes. *Comput. Chem. Eng.* **1989**, *13*, 73–82. [CrossRef]
13. Alhamad, B.; Romagnoli, J.A.; Gomes, V.G. On-line multi-variable predictive control of molar mass and particle size distributions in free-radical emulsion copolymerization. *Chem. Eng. Sci.* **2005**, *60*, 6596–6606. [CrossRef]
14. Garcia, C.E.; Morari, M. Internal model control.1. A unifying review and some new results. *Ind. Eng. Chem. Proc. Dd.* **1982**, *21*, 308–323. [CrossRef]
15. Park, M.J.; Rhee, H.K. Control of copolymer properties in a semibatch methyl methacrylate/methyl acrylate copolymerization reactor by using a learning-based nonlinear model predictive controller. *Ind. Eng. Chem. Res.* **2004**, *43*, 2736–2746. [CrossRef]
16. Gattu, G.; Zafiriou, E. Nonlinear quadratic dynamic matrix control with state estimation. *Ind. Eng. Chem. Res.* **1992**, *31*, 1096–1104. [CrossRef]
17. Lee, J.H.; Ricker, N.L. Extended kalman filter based nonlinear model-predictive control. *Ind. Eng. Chem. Res.* **1994**, *33*, 1530–1541. [CrossRef]
18. Henson, M.A. Nonlinear model predictive control: Current status and future directions. *Comput. Chem. Eng.* **1998**, *23*, 187–202. [CrossRef]
19. Schork, F.J.; Deshpande, P.B.; Leffew, W.K. *Control of polymerization reactors*; CRC Press: Boca Raton, FL, USA, 1993; pp. 101–104.
20. Crowley, T.J.; Choi, K.Y. Experimental studies on optimal molecular weight distribution control in a batch-free radical polymerization process. *Chem. Eng. Sci.* **1998**, *53*, 2769–2790. [CrossRef]
21. Ellis, M.F.; Taylor, T.W.; Jensen, K.F. Online molecular-weight distribution estimation and control in batch polymerization. *Aiche. J.* **1994**, *40*, 445–462. [CrossRef]
22. Congalidis, J.P.; Richards, J.R.; Ray, W.H. Feedforward and feedback-control of a solution copolymerization reactor. *Aiche. J.* **1989**, *35*, 891–907. [CrossRef]
23. Adebekun, D.K.; Schork, F.J. Continuous solution polymerization reactor control 2. Estimation and nonlinear reference control during methyl-methacrylate polymerization. *Ind. Eng. Chem. Res.* **1989**, *28*, 1846–1861. [CrossRef]
24. Florenzano, F.H.; Strelitzki, R.; Reed, W.F. Absolute, on-line monitoring of molar mass during polymerization reactions. *Macromolecules* **1998**, *31*, 7226–7238. [CrossRef]
25. Giz, A.; Catalgil-Giz, H.; Alb, A.; Brousseau, J.L.; Reed, W.F. Kinetics and mechanisms of acrylamide polymerization from absolute, online monitoring of polymerization reaction. *Macromolecules* **2001**, *34*, 1180–1191. [CrossRef]
26. Reed, W.F. Automated continuous online monitoring of polymerization reactions (acomp) and related techniques. *Anal. Chem.* **2013**. [CrossRef]
27. Baillagou, P.E.; Soong, D.S. Major factors contributing to the nonlinear kinetics of free-radical polymerization. *Chem. Eng. Sci.* **1985**, *40*, 75–86. [CrossRef]
28. Pinto, J.C.; Ray, W.H. The dynamic behavior of continuous solution polymerization reactors 7. Experimental-study of a copolymerization reactor. *Chem. Eng. Sci.* **1995**, *50*, 715–736. [CrossRef]
29. Ray, W.H. Mathematical modeling of polymerization reactors. *J. Macromol. Sci. R M C* **1972**, *8*, 1–56. [CrossRef]
30. Crowley, T.J.; Choi, K.Y. Calculation of molecular weight distribution from molecular weight moments in free radical polymerization. *Ind. Eng. Chem. Res.* **1997**, *36*, 1419–1423. [CrossRef]
31. Crowley, T.J.; Choi, K.Y. Optimal control of molecular weight distribution in a batch free radical polymerization process. *Ind. Eng. Chem. Res.* **1997**, *36*, 3676–3684. [CrossRef]
32. Ross, R.T.; Laurence, R.L. Gel effect and free volume in the bulk polymerization of methyl methacrylate. *Aiche. J.* **1976**, *72*, 74–79.

33. Fan, S.; Gretton-Watson, S.P.; Steinke, J.H.G.; Alpay, E. Polymerisation of methyl methacrylate in a pilot-scale tubular reactor: Modelling and experimental studies. *Chem. Eng. Sci.* **2003**, *58*, 2479–2490. [CrossRef]
34. Li, R.J.; Henson, M.A.; Kurtz, M.J. Selection of model parameters for off-line parameter estimation. *IEEE T Contr. Syst. T* **2004**, *12*, 402–412. [CrossRef]
35. Nowee, S.M.; Abbas, A.; Romagnoli, J.A. Optimization in seeded cooling crystallization: A parameter estimation and dynamic optimization study. *Chem. Eng. Process.* **2007**, *46*, 1096–1106. [CrossRef]